MAGNETOHYDRODYNAMICS Vol. 38 (2002), No. 1-2, pp. 5–14

DYNAMO EXPERIMENTS AT THE RIGA SODIUM FACILITY

A. Gailitis[1], *O. Lielausis*[1], *E. Platacis*[1], *S. Dement'ev*[1], *A. Cifersons*[1], *G. Gerbeth*[2], *Th. Gundrum*[2], *F. Stefani*[2], *M. Christen*[3], *G. Will*[3]

[1] *Institute of Physics, University of Latvia, Salaspils-1, LV-2169, Latvia*
[2] *Forschungszentrum Rossendorf, P.O. Box 510119, D-01314 Dresden, Germany*
[3] *Department of Mechanical Engineering, Dresden University of Technology, D-01062 Dresden, Germany*

We summarize the history and the results of the first successful hydromagnetic dynamo experiment which was prepared and run at the Institute of Physics in Riga, Latvia.

Introduction. Although known for at least two thousand years, the magnetic field of the Earth was a mystery until the beginning of the 20th century. Early rational attempts to understand the origin of this field attributed it to the "virtue" of the loadstone [1]. After Hale's discovery of the Sun's magnetic field in 1908 [2] the need for an alternative explanation of cosmic magnetic fields became evident. It was Larmor in 1919 [3] who paved the way for the modern hydromagnetic dynamo theory while explaining the solar magnetic field: "In this way it is possible for the internal cyclic motion to act after the manner of the cycle of a self-exciting dynamo, and maintain a permanent magnetic field from insignificant beginnings, at the expense of some of the energy of the internal circulation."

Dynamo theory of cosmic magnetic fields has come to maturity ever since. Nowadays, sophisticated numerical simulations are being carried out to understand in detail the strongly coupled behaviour of velocity and magnetic fields in cosmic bodies. Impressive similarities between the numerical results and observational facts have been found, culminating in the successful simulation of reversals of the Earth magnetic field [4]. However, these successes cannot obscure the fact that some of the parameters used in numerical simulations are still far away from those relevant to cosmic bodies. The actual relevance of the numerical results for the description of "natural" dynamos is, therefore, not completely clear.

Unfortunately, natural dynamos are also difficult to be investigated by observation. The dynamo of the Earth, for instance, works in the liquid outer core, in a depth between 2900 and 5200 km below the Earth's surface. Although the observed magnetic field does provide some information about its generation process, a lot of information is lost due to diffusion in the mantle which is not completely insulating.

Being restricted to analytical and numerical work without direct observational access to its subject, the science of hydromagnetic dynamos has been in an unsatisfactory state for decades. The long-cherished desire to build an experimental hydromagnetic dynamo was prevented by the large product of dimension and velocity which is necessary to reach the threshold of magnetic field self-excitation. This threshold was exceeded for the first time on 11 November 1999 at the dynamo facility in Riga [5] (see p. 4). A few weeks later self-excitation was achieved also on the dynamo facility in the Research Centre Karlsruhe, Germany [6].

The present paper is summarizing the essential aspects concerning the preparation and some of the most important results of the Riga experiment, keeping in mind that most of the material has already been published [5, 7, 8, 9].

1. Convective, absolute, and global instability. The basic idea of the Riga dynamo experiment traces back to a paper of Ponomarenko [10] who considered magnetic field self-excitation in an endless electrically conducting solid cylinder screwing rigidly through a medium at rest having the same conductivity. In this case, the magnetic field $\mathbf{B}$ depends exponentially on the axial coordinate z, the azimuthal angle ϕ and the time t: $\mathbf{B}(r, \phi, z, t) \sim \exp(pt + ikz + im\phi)$. The only non-trivial dependence becomes a radial one. In general, k and p are complex constants to be evaluated when the problem is solved. In our case the azimuthal mode corresponds to $m = 1$.

The magnetic field behaviour in fluids with conductivity σ and velocity field $\mathbf{v}$ is governed by the induction equation

$$\frac{\partial \mathbf{B}}{\partial t} = \nabla \times (\mathbf{v} \times \mathbf{B}) + \frac{1}{\mu_0 \sigma} \Delta \mathbf{B} \,, \tag{1}$$

where μ_0 denotes the permeability of the vacuum.

As a consequence of this equation the radial field dependence for Ponomarenko like dynamos results in Bessel functions of complex argument. Demanding continuity of electric and magnetic fields on contact surfaces and vanishing of the field on radial infinity, we get a closed complex and transcendent secular equation in a form

$$F(\mathrm{Rm}, k, p, \mathit{geometric\ parameters}) = 0 \tag{2}$$

having no analytic solution.

For high $\mathrm{Rm} = \mu_0 \sigma v_{max} R >> 1$ (v_{max} is the maximum velocity, R is the radius of the stream) an asymptotic solution gives some real k interval where the field is growing ($\Re\mathrm{e}\, p > 0$). For the experimentally more interesting region of smaller Rm Gailitis & Freibergs [11] had found that the field can grow if $\mathrm{Rm} > 17.7$ (numerical solution of (2) at optimum ratio of axial to azimuthal velocity). Such a growth of the field on infinite length is not equivalent with a growth in a limited space. The situation is called convective instability as all growing field perturbations are flowing downwards with some group velocity $\Re\mathrm{e}\,(i\partial p/\partial k)$ out of the module giving no feedback for the field generation. However, the group velocity can be modified and made close to zero by introducing a counterflow [12, 13, 14] which turns the convective instability into an absolute one. The zero group velocity as a saddle point in the complex $p(k)$ plane is a branching point in the inverse $k(p)$ plane. Hence close to it for any p there are two different k values k_1 and k_2. Two solutions moving in opposite directions can give the necessary feedback. Whereas this model is of infinite length, any real dynamo module has a finite length L. Within the framework of 1D calculations, the end effects can be approximatively taken into account by an asymptotic constraint $(k_1 - k_2)L = 2\pi$. It means that the generated field is a superposition of two solutions with the same time behaviour p, the same spatial growth rate $-\Im\mathrm{m}\, k$ and having the node separation equal to L. It looks like a standing wave deformed by a factor $\exp(-\Im\mathrm{m}\, kz)$. Solving together two secular equations (one with $k = k_1$, another with $k = k_2$) and the constraint one can get p, k_1 and k_2 for any Rm and arbitrary radial arrangements of flows. The method works for polynomial flow profiles in the central channel as well if self-definite power series are used instead of Bessel functions.

A complementary approach to the cylindrical dynamo problem was chosen by Stefani, Gerbeth and Gailitis [15]. In a time-dependent 2D solver the finite length

of the system was respected from the very beginning, hence the global instability can be computed directly. A central difference scheme was applied for the r and z dependence of the fields, and an Adams-Bashforth method of second order was used for the time evolution. In the outer part a Laplace equation was solved for every time step using a pseudo-transient method. It turned out that the results of this 2D solver differed only slightly from the results obtained with the 1D solver described above. The advantage of the 2D code is its applicability for velocity profiles which are varying along the z axis. The predictions for the growth rates and the frequencies where mainly computed using this 2D code.

2. Putting theory into practice. Many flows with a certain amount of helicity will result in magnetic field self-excitation if only the magnetic Reynolds number is made large enough. The actual problem is to build a dynamo with a reasonable financial and constructional effort.

Given the main flow topology indicated above, with a helical flow to amplify the magnetic field, a coaxial back-flow to ensure a positive feedback, and a third coaxial tube with sodium at rest to decrease the Ohmic losses, a number of optimization problems remained to be solved in order to get a working dynamo.

At first it was necessary to fix the basic geometric relations of the facility. Assuming a certain relation of different constructional and operational costs, this was done in [16].

Essential for the experiment was also the experience gained during the early (not fully successful) attempt to achieve self-excitation on a device which can be considered as a prototype to the present facility [14, 17, 18].

Fig. 1 shows schematically the final design of the dynamo. Besides the central module with three coaxial cylinders filled with sodium, the main parts are two 55 kW motors, a propeller with tailored pre- and post-propeller vanes and sodium storage tanks. The total amount of sodium used in the experiment is 2 m^3. The velocity can reach values of about 15 m/s, allowing a flow rate of the order 0.6 m^3/s.

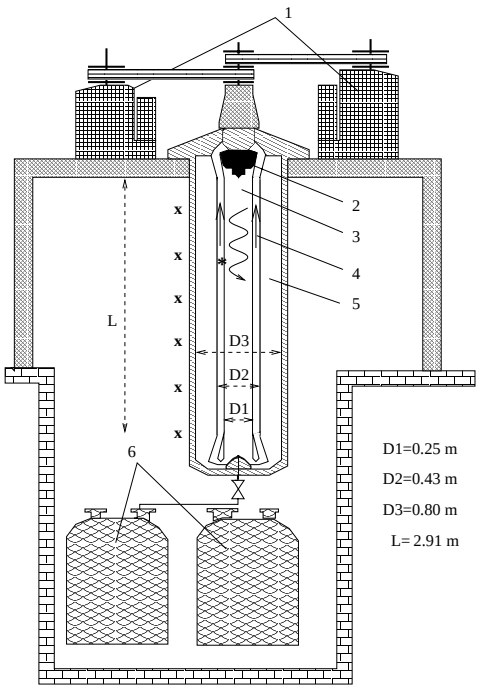

Fig. 1. The Riga dynamo facility. Main parts are: *1* – two motors (55 kW each), *2* – propeller, *3* – helical flow region, *4* – back-flow region, *5* – sodium at rest, *6* – sodium storage tanks, $*$ – position of the flux-gate sensor F, **x** – positions of the six Hall sensors.

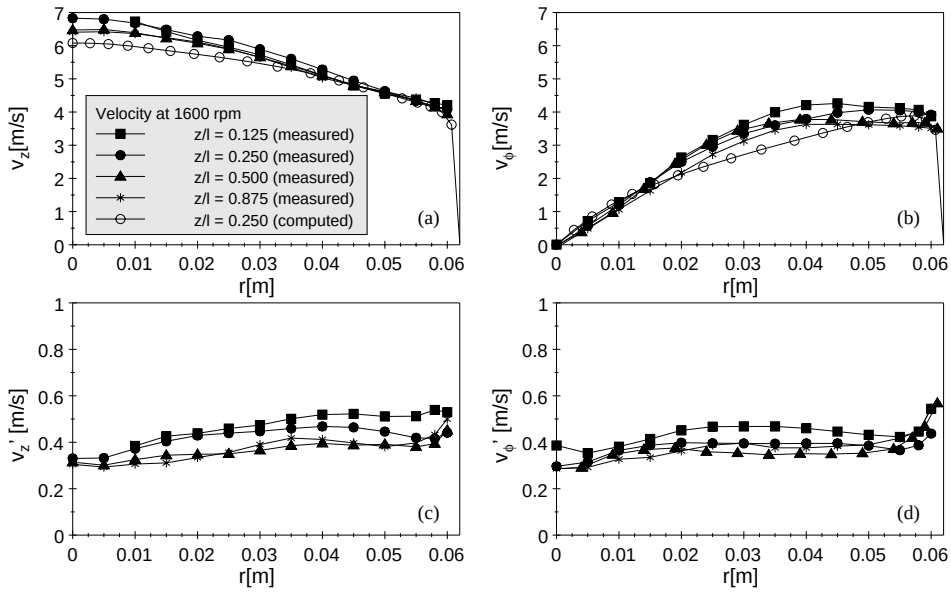

Fig. 2. Velocity profiles measured at a 1:2 water test model at the Dresden University of Technology. The flow structure can be considered as equivalent with the real flow at the Riga facility. Measured mean axial (a) and azimuthal (b) components at different distances from the propeller, and the corresponding fluctuations (c) and (d).

Five years were devoted to the installation of a full size water test facility and of the final sodium facility. One aspect of those pre-experiments was to ensure the mechanical integrity of the system, particularly with respect to keep the innermost stainless steel wall as thin as possible (1.5 mm) in order to minimize Ohmic losses. A lot of effort has been put into vibrational measurements at the water facility [19] and into simulations of the fluid-structure interaction resulting in a careful design of the fixing elements of the tubes.

The test runs with water turned out crucial for the success of the later sodium experiments as it was necessary to optimize the velocity profiles in order to reach self-excitation within the given motor power limitations. One of the results of the optimization was that using helicity maximizing functions (Bessel functions J_0 for the axial and J_1 for the azimuthal velocity component) the critical magnetic Reynolds number could be reduced by about 20% in comparison with the usual solid body rotation profile.

The iterative process of theoretical and numerical profile optimization [15], pump design and velocity measurements [20] was finished in 1998.

In connection with this, a 1:2 water model of the hydraulic part of the dynamo was build at the Technical University of Dresden. Using Laser-Doppler-Velocimetry, this model allowed to study the mean velocity fields and the turbulent fluctuations in more detail than in the real facility.

Fig. 2 shows the axial (a) and the azimuthal (b) velocity profiles and the corresponding fluctuations (c, d) measured in the central tube of this 1:2 water model. The velocity profiles differ significantly from the solid body rotation profiles. Of course, the theoretically desired Bessel flow profiles cannot be achieved in the real hydraulic device, but they are tailored as close as possible in this sense. Note the far-reaching constancy of the mean velocity along the z-axis. Due to continuity

demand, this is not astonishing for the axial component. For the azimuthal component, this effect of inertia is remarkable. Apart from an overall scaling factor, these profiles can be considered as reasonable approximations of the flow in the real sodium device. As turbulence is less than 10% of the mean flow it has negligible influence on generation conditions.

Until the first sodium experiment could start, it took again more than a year to finish all necessary preparations.

3. The first experiment in November 1999. A first series of experiments was carried out during 6–11 November 1999. After having filled the whole dynamo module, sodium was pumped slowly through the channels at 300°C for 24 hours in order to ensure good electrical contact between the walls and the sodium. The main experiment was planned at a temperature of about 150°C. While cooling down from 300°C to 150°C, two pre-experiments where planned at 250°C and 200°C. At 250°C, self-excitation was not expected to occur. At 200°C this question was open. Unfortunately, after the last run at about 210°C the experiment had to be stopped due to some technical problems with a seal.

The main purpose of these pre-experiments was to test the response of the dynamo on an externally applied magnetic field which was produced by seed field coils fed by a 3-phase current of variable low frequency (Fig. 3). Fig. 4 shows the inverse ratio of the measured magnetic field to the applied current in the seed field coils for a feeding frequency of 1 Hz versus the rotation rate of the propeller. An increasing amplification of the seed field can clearly be identified until a rotation rate of 1800 rpm. Above this value, the amplification slightly decreases which has to do with the passing of the eigenfrequency of the dynamo. Note that all points in Fig. 4 except the rightmost cross were derived from very clean sinusoidal signals

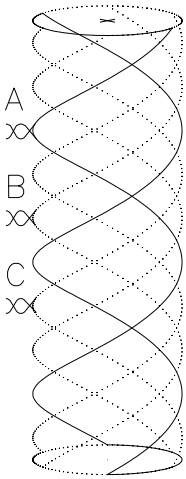

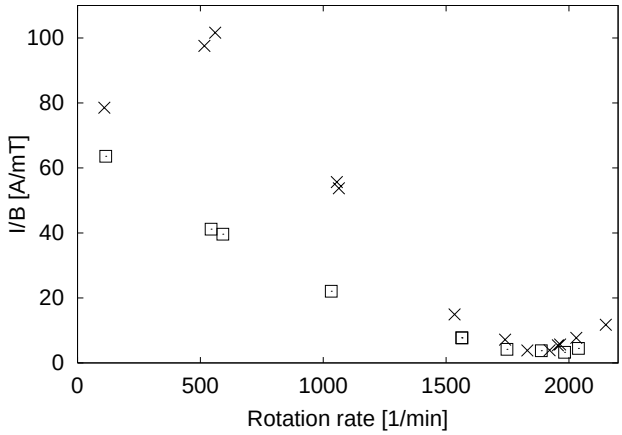

Fig. 3. Three phase coil wound around the dynamo module. The geometry of the seed field resulting from this coil is similar to the geometry of the eigenmode of the dynamo. The same coil was used as a measuring device giving an integral value of the generated magnetic field.

Fig. 4. Magnetic field amplification in dependence on the propeller rotation rate for seed field frequency $f = 1$ Hz. The ordinate axis shows the inverse ratio of the measured magnetic field to the current in the seed field coils. Squares and crosses correspond to two different settings of the 3-phase current in the seed field coils with respect to the propeller rotation.

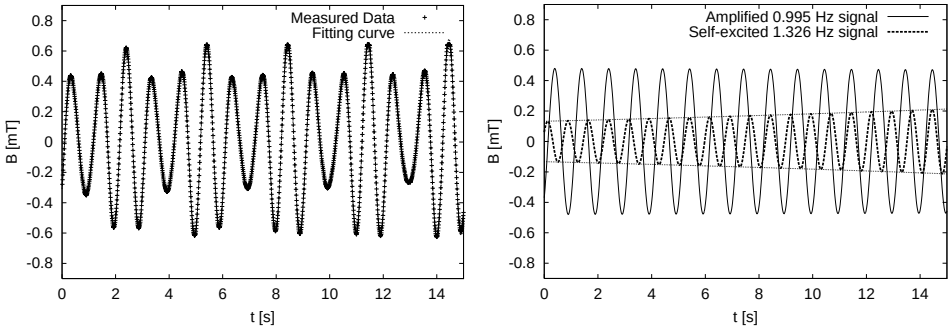

Fig. 5. Magnetic field signal measured at 2150 rpm at the flux gate sensor F and fitting curve (left). Decomposition of the fitting curve into two curves with different frequencies (right). The growth rate of the 1.326 Hz signal was $p = +0.03s^{-1}$.

of the same 1 Hz frequency as the seed field. In this regime, there is a strong amplification without self-excitation. Switching off the current in the seed field coils, the magnetic field decays [5].

Consider now the rightmost cross in Fig. 4. At this rotation rate (2150 rpm), a new sort of signal was recorded which is shown in Fig. 5. This signal can be decomposed, with a high statistical significance [5], into the usual amplified 1 Hz signal and another signal with a different frequency which is exponentially increasing (Fig. 5*b*).

Our interpretation of the signal shown in Fig. 5 was that it is a superposition of two *independent* magnetic field modes which are clearly identifiable by their frequencies. Of course, in order to explain the amplitude of the 1.3 Hz mode one has to consider that during the last acceleration phase (before the rotation rate had reached the maximum of 2150 rpm) a mixture of frequencies was born out of the 1 Hz mode due to the time dependence of the velocity. After this acceleration phase, however, the mixture of modes evolved in agreement with kinematic dynamo theory: the 1 Hz mode continued to be amplified, and all modes with different frequencies showed the usual exponential time dependence. All but one modes were decaying. Only the mode with the eigenfrequency of the dynamo at the reached rotation rate survived and continued to grow exponentially. The above interpretation was fully confirmed in the second experiment.

4. The second experiment in July 2000. In July 2000 it was possible to work at considerable lower sodium temperatures (around 160°C and thus at higher Rm. Fig. 6 gives an overview about the four runs which were carried out during 22-25 July 2000. In each of the plots the rotation rates as well as the magnetic field signals recorded at one Hall sensor (the fourth sensor from above in Fig. 1) are shown. Fig. 6*a* illustrates the first run at a temperature of about 210°C. Intended mainly as a test, this run was carried out completely in the subcritical regime; the shown signal is therefore always the amplified 1 Hz signal of the seed field coils. The next three runs were carried out at temperatures around 160°C. Figs 6*b, c* contain periods with and without seed field. Perhaps the clearest run is documented in Fig. 6*d* where no seed field was used at all. Here it is shown how the signal "emerges from nothing" after the rotation rate has reached a critical value (approximately 1920 rpm) and how the field amplitude saturates at levels dependent on the rotation rate.

Some more details from the start and the end of this run are depicted in Fig. 7 where the signal recorded by the much more sensitive inner flux gate sensor

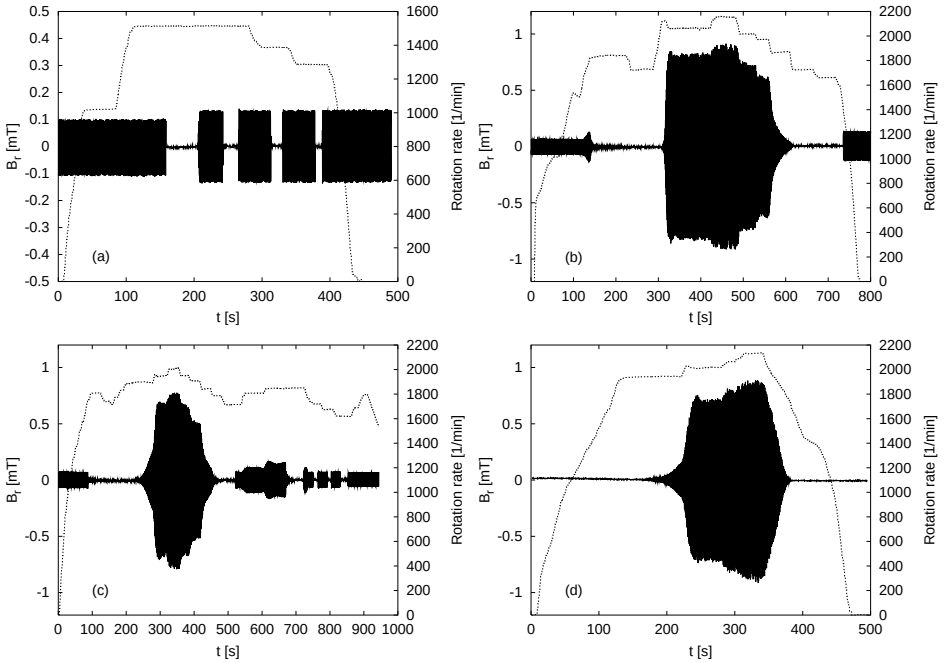

Fig. 6. Four experimental runs in July 2000. Rotation rate of the motors, and magnetic field measured at one Hall sensor (the fourth from above in Fig. 1). First test run (a) at 210°C without self-excitation; the recorded field is the amplified field of the seed field coils. In (b) and (c) there are periods with and without seed field. The large amplitude signals are recorded during self-excitation. In (d) the seed field coils were switched off during the whole run.

(the star in Fig. 1) is plotted. The first interesting detail here is how the Earth's magnetic field is "pushed out" of the dynamo when the rotation rate runs from 500 to 1000 rpm (Fig. 7a) and how it "comes back" again when the rotation rate is decreasing at the end of the run (Fig. 7b). This behaviour is nothing else than the usual skin effect. The most interesting detail is the self-excitation of a rotating magnetic field which is clearly seen to start at $t = 130$ s.

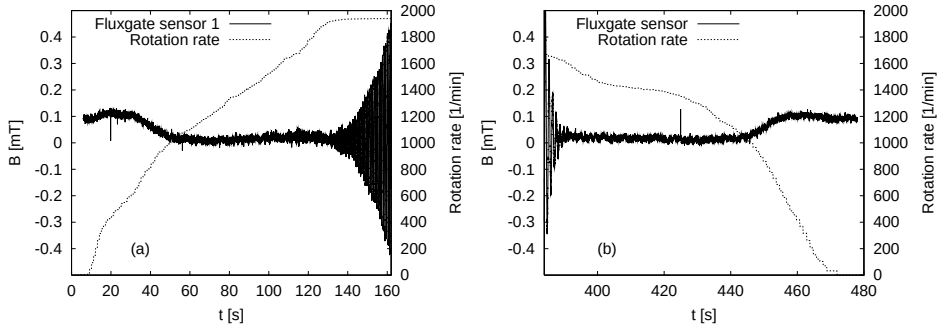

Fig. 7. Measured magnetic field at flux-gate sensor. Details at the beginning and at the end of the run in Fig. 6d. Pushing out (a) and "coming back" (b) of the Earth's magnetic field, as well as the beginning of the self-excitation (a).

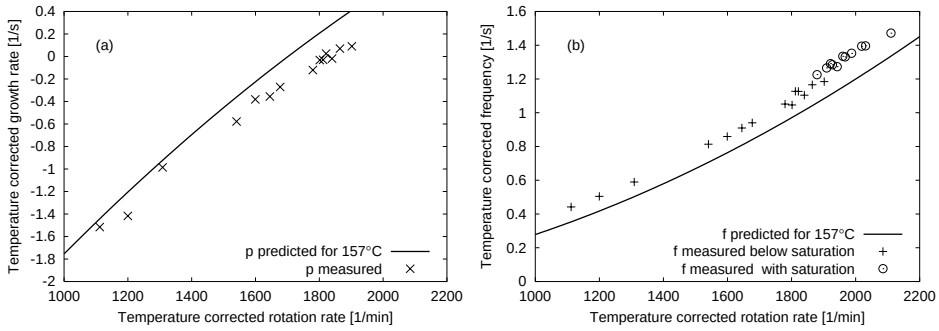

Fig. 8. Growth rates (a) and frequencies (b) measured in November 1999 and July 2000 experiments for different rotation rates and temperatures, and corresponding numerical predictions. The propeller rotation rate Ω as well as the growth rate p and the frequency f at the temperature T were scaled to $(\Omega_c, p_c, f_c) = \sigma(T)/\sigma(157^\circ C)\,(\Omega(T), p(T), f(T))$. In ($b$) the frequencies in the saturation regime are also given, whereas the corresponding growth rates are zero.

5. Comparison with predictions. From all experimental runs conducted in November and July, we have assembled in Fig. 8 the measured growth rates (a) and frequencies (b) in dependence on the rotation rate. We have taken into account only those time intervals where the rotation rate was kept constant. Most of the data were recorded during field decays after the seed field had been switched off. A few points with positive growth rate correspond to the kinematic phase of self-excitation when the saturation regime had not been reached yet. Only in the frequency plot in Fig. 6*b*, there are also some points in the saturation regime which will concern us below.

As for the growth rates and the frequencies in the kinematic regime, the correspondence of the measured data and the predicted curves is quite convincing. Notable is a slight shift of the measured growth rate data of about 10 % towards higher rotation rates and an overall shift of the frequency data of about 5 % towards lower rotation rates. In both cases the slopes of the curves are in good agreement with the predictions.

It is interesting that the frequency in the saturation regime is not very different from what would be expected from simply extrapolating the kinematic regime, whereas the growth rate in the saturation regime goes to zero. This is a surprising fact as it indicates that there must be a significant deformation of the fluid velocity apart from an overall pressure increase due to the Lorentz forces.

More details about the saturation regime and preliminary interpretations can be found in [21].

6. Conclusions and prospects. After years of preparation, including the well-aimed determination of the overall flow geometry, the design of the whole facility with careful considerations of all requirements of sodium technique, and experimental fine-tuning of the velocity profiles based on extensive computer simulations, the Riga dynamo has turned out as a neatly working hydromagnetic facility. It is well-predictable in the kinematic regime, and it shows already a non-trivial behaviour in the saturation regime. The whole installation is ready for a number of additional experiments in which the back-reaction and the MHD turbulence can be studied.

Acknowledgments. We thank the Latvian Science Council for support under grants 96.0276 and 01.0502, the Latvian Government and International Science Foundation for support under joint grant LJD100, the International Science Foundation for support under grant LFD000 and the Deutsche Forschungsgemeinschaft for support under INK 18/B1-1. We are grateful to W. Häfele for his interest and support, and to the whole experimental team for preparing and running the experiment.

REFERENCES

1. W. Gilbert. *De magnete.* (Dover, New York, 1991).
2. G.E. Hale. *The Study of Stellar Evolution.* (University of Chicago Press, Chicago, 1908).
3. J. Larmor. How could a rotating body such as the sun become a magnet? *Rep. Brit. Assoc. Adv. Sci.* (1919), pp. 159–160.
4. G.A. Glatzmaier, P.H. Roberts. A three-dimensional self-consistent simulation of a geomagnetic field reversal. *Nature* vol. 377, pp. 203–209.
5. A. Gailitis, O. Lielausis, S. Dement'ev, E. Platacis, A. Cifersons, G. Gerbeth, Th. Gundrum, F. Stefani, M. Christen, H. Hänel, G. Will Detection of a flow induced magnetic field eigenmode in the Riga dynamo facility. *Phys. Rev. Lett.*, vol. 84 (2000), pp. 4365–4368.
6. R. Stieglitz, U. Müller Experimental demonstration of a homogeneous two-scale dynamo. *Phys. Fluids*, vol. 13 (2001), pp. 561–564.
7. A. Gailitis, O. Lielausis, E. Platacis, S. Dement'ev, A. Cifersons, G. Gerbeth, Th. Gundrum, F. Stefani, M. Christen, G. Will Magnetic field saturation in the Riga dynamo experiment. *Phys. Rev. Lett.*, vol. 86 (2001), pp. 3024–3027.
8. A. Gailitis, O. Lielausis, E. Platacis, G. Gerbeth, F. Stefani On the results of the Riga dynamo experiments. *Magnetohydrodynamics*, vol. 37, No. 1/2, pp. 71–80.
9. A. Gailitis, O. Lielausis, E. Platacis, G. Gerbeth, F. Stefani Riga dynamo experiment. in: *Dynamo and dynamics, a mathematical challenge*, edited by P. Chossat, D. Armbruster, I. Oprea, Kluwer Academic Publishers, Dordrecht (2001), pp. 9–16.
10. Yu.B. Ponomarenko. On the theory of hydromagnetic dynamo. *J. Appl. Mech. Tech. Phys.* vol. 14 (1973), pp. 775–779.
11. A. Gailitis, J. Freibergs. To the theory of a helical MHD-dynamo. *Magnetohydrodynamics*, vol. 12 (1976), pp. 127–129.
12. A. Gailitis, J. Freibergs. Nature of instability in a helical MHD dynamo. *Magnetohydrodynamics*, vol. 16 (1980), pp. 116–121.
13. A. Gailitis. The Helical MHD Dynamo. In: *Topological Fluid Mechanics Proc. IUTAM Symposium, Cambridge, 1989 August 13-18.*, edited by H.K. Moffatt and A. Tsinober Cambridge UP pp. 147–156.
14. A. Gailitis, B.G. Karasev, I.R. Kirillov, O.A. Lielausis,, A.P. Ogorodnikov. The Helical MHD Dynamo. In: *Liquid Metal Magnetohydrodynamics*, edited by J. Lielpeteris and R. Moreau, Kluwer AP, Dordrecht 1989 pp. 413–419.
15. F. Stefani, G. Gerbeth, A. Gailitis. Velocity profile optimization for the Riga dynamo experiment. In: *Transfer Phenomena in Magnetohydrodynamic and Electroconducting Flows*, edited by A. Alemany, Ph. Marty, J. P. Thibault, Kluwer Academic Publishers, Dordrecht (1999), pp. 31–44.
16. A. Gailitis. Project of a liquid sodium MHD dynamo experiment. *Magnetohydrodynamics*, vol. 32 (1996), pp. 58–62.

17. A. Gailitis, B.G. Karasev, I.R. Kirillov, O.A. Lielausis, S.M. Luzhanskii, A.P. Ogorodnikov, G.V. Preslitskii. A liquid metal MHD dynamo model experiment. *Magnetohydrodynamics*, vol. 23 (1987), pp. 349–353.

18. A. Gailitis. Experimental aspects of a laboratory scale liquid

    sodium dynamo model In: *Proceedings of NATO ASI "Theory of Solar and Planetary Dynamos" 20.IX-2.X 1992 Cambridge, U.K.*, edited by M.R.E. Proctor, P.C. Matthews and A.M. Rucklidge, Cambridge UP, pp. 91–98.

19. E. Altstadt. Internal report. FZ Rossendorf (1997).

20. M. Christen, H. Hänel, G. Will. Entwicklung der Pumpe für den hydrodynamischen Kreislauf des Rigaer "Zylinderexperimentes". In: *Beiträge zu Fluidenergiemaschinen 4*, edited by W. H. Faragallah, G. Grabow, Faragallah-Verlag und Bildarchiv, Sulzbach/Ts. (1998), pp. 111–119.

21. A. Gailitis, O. Lielausis, E. Platacis, G. Gerbeth, F. Stefani. On back-reaction effects in the Riga dynamo experiment. *Magnetohydrodynamics*, vol. 38 (2002), no. 1-2, pp. 15–26.

Received 24.09.2001